Infinite Science | Publishing

Peridynamic investigation of surface cracks in optimality criterion-based topology optimization for additive manufacturing

Abdullah Kendibilir[1,2,3]*, Mahmut Hudayi Bilgin[1,2,3], Adnan Kefal[1,2,3]*

[1] *Faculty of Engineering and Natural Sciences, Sabanci University, Tuzla, Istanbul 34956, Turkey*
[2] *Composite Technologies Center of Excellence, Sabanci University-Kordsa, Istanbul Technology Development Zone, Sanayi Mah. Teknopark Blvd. No: 1/1B, Pendik, 34906 Istanbul, Turkey*
[3] *Integrated Manufacturing Technologies Research and Application Center, Sabanci University, Tuzla, 34956, Istanbul, Turkey*
* *Corresponding author: adnankefal@sabanciuniv.edu (A. Kefal)*

Abstract

Topology optimization (TO) is extensively used for reducing the weight of engineering parts that require higher performance in aerospace, automotive, and defense industries. Additive manufacturing (AM), a practical layer-by-layer material deposition process, is commonly employed to fabricate geometrically complex designs obtained from TO. However, AM processes may result in manufacturing-induced structural discontinuities (surface cracks or voids) that must be considered in the design stage. Nevertheless, most TO algorithms cannot realistically handle these structural cracks/defects since they mainly employ classical continuum-mechanics formulations combined with the finite element method (FEM). On the other hand, peridynamics (PD), a non-local meshless approach, can effectively model any structural discontinuity without the need for an additional effort by breaking non-local interactions. In this study, we combine PD and optimality criterion-based TO methods to investigate the effect of surface cracks on the three-dimensional structural design. For a comparative study, these cracks are also modeled using FEM-TO by eliminating the elements in the cracked region. Optimal geometries and total strain energies obtained from PD are compared with those from FEM for the benchmark case with/without surface cracks. Finally, the advantage of PD is revealed for modeling structural discontinuities in TO.

Keywords: Topology optimization, peridynamics, crack modelling, additive manufacturing, finite element method.

1. Introduction

Most of the engineering structures used in automotive, aerospace, and other manufacturing industries are desired to be lightened by utilizing novel design tools [1-6]. In this context, topology optimization (TO) methods have been dedicated to decreasing the weight of the critical engineering structures while minimizing compliance of the structure. Numerous TO methods have been proposed in recent decades.

Among various TO algorithms, the solid isotropic material with penalty (SIMP) method [7-9] was originally proposed by Bendsoe which relaxes the originally ill-posed TO problem by using continuous design variables. Another popular TO method, Evolutionary structural optimization (ESO) [10, 11], has been used for a variety of topology and shape optimization problems. In addition, the additive ESO (AESO) method [12] creates a structure that expands from a basis connecting the domain between the supports and loads. On the other hand, as a combination of ESO and AESO techniques, the bi-directional evolutionary structural optimization (BESO) method [13-15] can add or remove the material during the optimization. Apart from these techniques, a variety of optimization methods such as ground structure [16], level-set [17, 18], moving morphable void [19], and

moving asymptotes methods [20, 21] have been proposed.

While TO methods updates the material distribution, the structural integrity is analyzed in each step. Therefore, structural analysis methods have been combined with optimization algorithms. Here, the finite element method (FEM) which is a local classical continuum mechanics (CCM) formulation has been preferred by many researchers. However, most of the well-known methods do not consider structural discontinuities during optimization. Topologically optimized structures are generally fabricated by additive manufacturing due to their complexity and they are prone to crack initiation during manufacturing or operation due to heating and cooling repeatedly [22, 23]. Therefore, the ability to realistically embed cracks into the design domain during optimization is crucial to making topologies more resistant to such process-induced defects.

Mesh-based methods such as FEM require re-meshing for the simulation of cracked structures which is cumbersome in case of a complex discontinuity. Moreover, classical continuum mechanics formulation uses spatial differential equations which is prone to inaccurate results in the presence of structural discontinuities. Alternatively, meshless methods have

been proposed to eliminate the complexities related to the mesh. Some of the meshless methods utilized in topology optimization are the element-free Galerkin method (EFG) [24] and the smoothed particle hydrodynamics method (SPH) [25].

Peridynamics, a meshless method proposed by Silling [26-28], is a capable tool to overcome mesh-associated issues. PD is a bond-based local formulation that utilizes integro-differential equations, unlike CCM. Without re-meshing, any structural discontinuity can be embedded by breaking the relevant bonds in PD thereby represented realistically with less computational effort relative to mesh-based methods. PD is coupled with TO first in [29] using BESO and extended to continuous density-based PD-TO in [30]. Both studies investigated the TO of cracked structures using PD. In addition, 2D PD and FEM are compared for TO of cracked structures in [31, 32], and the advantages of PD in presence of structural discontinuities are revealed. Moreover, PD-TO is performed for reducing the weight of marine structures in [33].

To the best of the authors' knowledge, there is no comparative study on PD-TO and FEM-TO of 3D cracked structures in the literature. Therefore, we mainly focus on the investigation of the effective modeling of cracks and compare the performance of PD-TO and FEM-TO in 3D. This paper is organized as follows. PD theory, TO problem, and crack involvement methods are briefly discussed in section 2. Then, the selected case study is described, and its results are presented in section 3 which is followed by the conclusion.

2. Material and methods

2.1. Peridynamics Formulation for Structural Analysis

The general PD equation of motion for a material point located at x can be written as follows:

$$\rho(x)\ddot{u}(x,t)=\int_{H_x}\begin{pmatrix}t(x'-x,u'-u)\\-t'(x-x',u-u')\end{pmatrix}dH_x+b(x,t) \quad (1)$$

In the PD domain, each material point or particle can only interact with its family points which are the members of its horizon (H_x) with a radius of δ for a two- or three-dimensional body. The extent of a point can be a circle or sphere in 2-D and 3-D domain, respectively. In Eq. (1), ρ is the density of particle where $\ddot{u}$ represents the acceleration. Moreover, b corresponds to body force acting on a particle and t is the force density vector. This vector can be calculated as follows:

$$t(x'-x,u'-u)\equiv t(\xi,\eta)=\frac{1}{2}f(\xi,\eta)\frac{y'-y}{|y'-y|}\equiv f(\xi,\eta) \quad (2)$$

where f represents the magnitude of the pairwise force density vector, f. Additionally, we should define

the terms ξ and η which are corresponding to relative position and displacement vector, respectively.

$$\xi=x'-x \text{ and } \eta=u'-u \quad (3)$$

Note that the final position vector of x can be defined as $y=x+u$. To be able to measure the compliance of the body, we need to calculate the strain energy densities of each particle. Therefore, the first step should be to know the micro-potential of each PD bond. Hence, one can integrate the micro-potential of each interaction of a particle to be able to calculate the strain energy density of the particle. The micro-potential of each bond can be given by:

$$w(\xi,\eta)=\frac{1}{2}f(\xi,\eta)(|\xi+\eta|-|\xi|)\equiv\frac{1}{2}cs^2|\xi| \quad (4)$$

where $c=12E/\pi\delta^4$ is the bond constant for a three-dimensional isotropic material, and $s=|\xi+\eta|/|\xi|-1$ is the stretch between two particles. Then, integrating the micro-potential over a particle gives the strain energy density:

$$W(x,t)=\frac{1}{2}\int_{H_x}w(\xi,\eta)dH_x \quad (5)$$

Finally, one can find the compliance of the whole structure by summing particle-wise strain energy densities (calculated in Eq. 5) as given in the following:

$$C=\int_{\beta}W(x,t)d\beta \quad (6)$$

Compliance of the structure C should be minimized since it has been determined as objective function of the topology optimization problem. After the assembly process, the PD equation of motion can be resulted as a single matrix-vector form in the global domain β as :

$$\mathbf{KU}=\mathbf{F} \text{ , where } \mathbf{K}=\bigcup_{i=1}^{N}k_i, \quad \mathbf{U}=\bigcup_{i=1}^{N}u_i, \quad \mathbf{F}=\bigcup_{i=1}^{N}f_i \quad (7)$$

The global stiffness matrix, $\mathbf{K}$, displacement vector, $\mathbf{U}$, and the force vector $\mathbf{F}$ in the global system can be produced by assembling of local stiffness matrix k_i, displacement vector u_i, and force vector, f_i, respectively.

2.2. Optimization Procedure and Optimality Criteria Method

Minimization of compliance in TO can be described in a general form as follows:

$$\min_{\kappa} C(\kappa_i)\equiv C=\sum_{i=1}^{N}W(\mathbf{x}_i)V_i \text{ s.t.} \begin{cases} \mathbf{KU}=\mathbf{F} \\ \dfrac{\sum_{i=1}^{N}\kappa_i V_i}{\sum_{i=1}^{N}V_i}=\bar{V} \\ 0\leq\kappa(x)\leq 1,\forall x\in\beta \end{cases} \quad (8)$$

For the solution of structural analysis (KU=F), we utilize two different approaches: PD and FEM. For discretization, FEM mesh includes eight-noded hexahedral elements whereas PD creates equally spaced uniform material particles. The optimality criteria method is selected for the design variable updating scheme during the optimization process [34-35]. To describe the elastic modulus of particles individually, the power-law interpolation scheme is explained as follows:

$$E_i \equiv E_i(\kappa_i) = E^v + (\kappa_i)^p (E^s - E^v) \qquad (9)$$

Here, E^v and E^s correspond to material properties of void and solid materials. Moreover, p, is referred to the "penalization factor" to find discrete design variables. One can set $E^v = 0$ and change the design variable of a void particle from zero to a relatively close positive number by doing so. This results in the following form of the equation:

$$E_i = (\kappa_i)^p E^s \qquad (10)$$

For solid and void particles, respectively, design variables $\kappa_i = 1$ and $\kappa_i = \kappa_{min}$ are defined in the equation above. We selected penalty parameter and minimum density value as $p = 3$ and $\kappa_{min} = 10^{-3}$, respectively. In the OC method, the design variable updating scheme works as:

$$\kappa_i^{new} = \begin{cases} \max(0, \ \kappa_i - mv) \\ if \quad \kappa_i B_i^{0.5} \leq \max(0, \ \kappa_i - mv) \\ \min(1, \ \kappa_i + mv) \\ if \quad \kappa_i B_i^{0.5} \geq \min(1, \ \kappa_i + mv) \\ \kappa_i B_i^{0.5} \quad otherwise \end{cases}, \text{where } B_i = \frac{-\dfrac{\partial C(k_i)}{\partial k_i}}{l \dfrac{\partial V(k_i)}{\partial k_i}} \qquad (11)$$

Where mv is the move limit, and bisection approach can be used to determine the suitable value of l (Lagrangian multiplier).

2.3. Crack Involvement in PD and FEM

Since the main motivation of this study is reducing the weight of cracked structures using two different TO methods (FEM-TO and PD-TO), crack modelling should be clarified by giving fundamental differences between these methods. Therefore, Fig. 1 gives a representative example of the crack involvement procedure and its effect on the problem domain. If the crack surface passes through certain elements in the discretized domain by FEM, Figure 1a shows that the elements which coincide with the crack involved need to be deleted. Although the mesh is uniformly distributed in this example, an engineering structure in real-life could be more sophisticated, and thus remeshing or some other treatments may be needed. This strategy also alters the original geometry by deleting the relevant elements which causes additional mistakes due to the missing representation of the problem. To better represent a discontinuity, using denser mesh would be logical. After that, computational time will increase

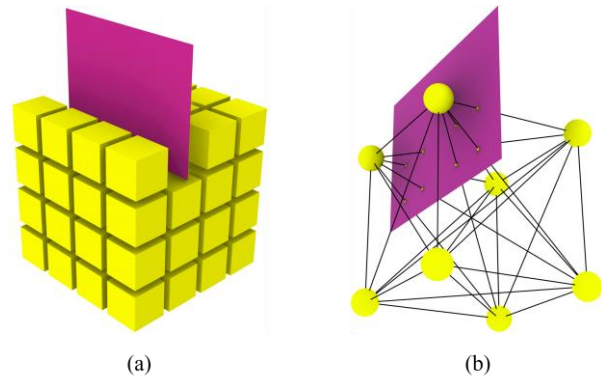dramatically. As a result, crack modeling may not be practical for FEM analysis.

(a)   (b)

Fig 1. Illustrations of crack modeling strategy of (a) FEM and (b) PD.

3. Results and discussion

For a meaningful comparison of the PD-TO and FEM-TO methods, we selected a well-known benchmark TO problem from the literature. We modeled an L-beam geometry as shown in **Fig. 2** where the length of L=1m. The top surface of the structure is fully clamped while a downward concentrated force F=50 kN is applied to the middle of the edge as depicted in Figure 2. In the PD analysis, the force is applied as body force density to two PD particles equally. Moreover, for the FEM analysis, the force is distributed to three nodes to be able to apply the same loading condition in both methods.
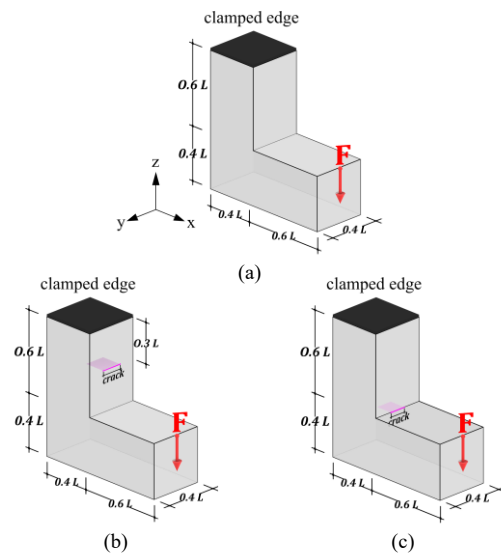

Fig 2. Design domain and boundary conditions for an L-beam; (a) without crack (b) with a crack in the upper region and (c) with a crack in the middle region.

The problem domain and its discretized versions for the FEM and PD analyses are demonstrated in Fig. 3. Here, the domain is discretized into 60x24x60 material particles for PD analysis or elements for FEM analysis in the x-y and z directions, respectively. It means that the

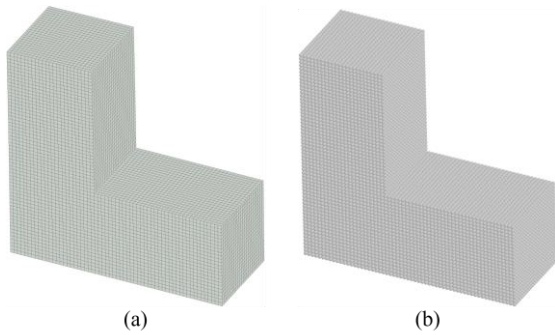distance between two particles is dx=1/60 m in the PD model.

Fig 3. Spatial discretization of the problem domain using (a) FEM and (b) PD.

However, the FEM model consists of eight-noded hexahedral elements with an edge of the length of dx particle size. Hence, the discretized domain contains 55296 particles/elements in total. The target volume after optimization is set to 20% of the initial volume of the structure.
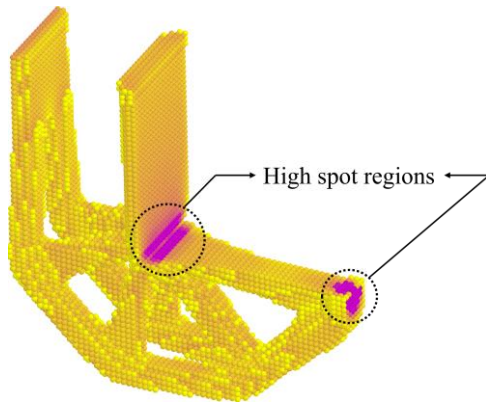

Fig 4. Strain energy density distribution for crack-free state of the problem domain.

Moreover, elastic modulus and Poisson's ratio of the material are set to E=200 GPa and v=0.25, respectively. Without changing the problem constraints and material properties, we embedded surface cracks into the problem domain in two different positions as illustrated in Figures 2b and 2c. The varying locations are chosen to compare the effect of crack involvement on the PD-TO and FEM-TO. Before the crack locations are determined, the strain energy density distribution is examined for the scenario without a crack.
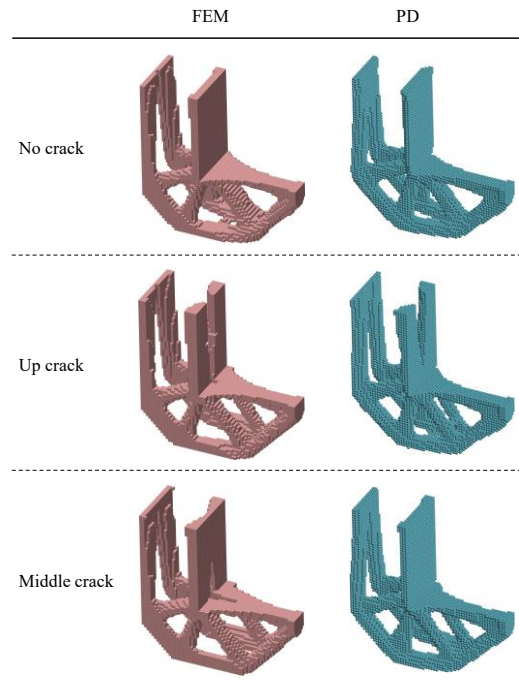

Fig 5. Optimal topologies obtained by FEM-TO and PD-TO for varying crack scenarios.

The strain energy distribution of the crack-free case is given in Fig. 4. Here, high-spot regions where the particles with the highest strain energy are accumulated can be investigated. Accordingly, we determine two different crack locations which have high and low strain energy density. As can be seen, the up crack is embedded into a safer region than the crack in the middle region. A squared-shape surface crack located on the upside of the geometry has an $10 \times dx$ edge length, whereas the middle crack has an edge length of $8 \times dx$.

The final topologies after optimization for all the cases with and without cracks are presented in Fig 5. Here, the left and right columns contain FEM-TO and PD-TO results, respectively. The methods resulted in similar geometries in the case of the scenario without crack. In addition, the reactions of PD-TO and FEM-TO in up-crack cases are very close. In this case, both methods split the thick arm at the right bottom into two thinner branches and opened the normal direction of the crack. However, the branches in the PD-TO result are closer, and the opened region is deeper in the FEM-TO result. On the other hand, besides splitting the thick arm, the methods reacted differently in the middle crack area as shown in the last row in Fig. 5. FEM-TO eliminated a significant amount of material in the normal direction of the crack while there is no such effect in the PD-TO result.

Infinite Science | Publishing

Table 1. Compliance comparison.

Crack scenario	FEM results [Nm]	PD results [Nm]	Percent Diff. (%)
No crack	6.664	6.640	0.36
Up crack	6.783	6.724	0.87
Middle crack	6.707	6.567	2.09

Table 1 presents a comparison of FEM-TO and PD-TO in terms of the compliance results of the topologically optimized structures. In all cases with and without cracks, PD-TO provides a slightly better compliance value as compared to FEM-TO. The percent difference varies between 0.35 and 2.10 for the three cases. Moreover, PD-TO achieved even less compliance with the middle crack case relative to the scenario without crack while FEM-TO resulted in higher compliance with each crack. Between two crack scenarios, the reactions of the methods and the compliance results show that PD has an advantage in the case of a crack located in a critical region and it considers the whole structure during optimization due to its non-local nature while FEM mostly prioritizes changing the crack region. Moreover, the total displacement distributions are depicted in Fig. 6 with the maximum values. It is shown that displacement values are close to each other for the cases without crack and up-crack. However, for a critical crack position, PD-TO provides a better displacement value as compared to FEM-TO. Consequently, PD is observed to be capable of reducing the total compliance and total displacements of topologically optimized structures when cracks are embedded into high-strain energy regions where structural discontinuities are expected to occur when the structure is manufactured and loaded.
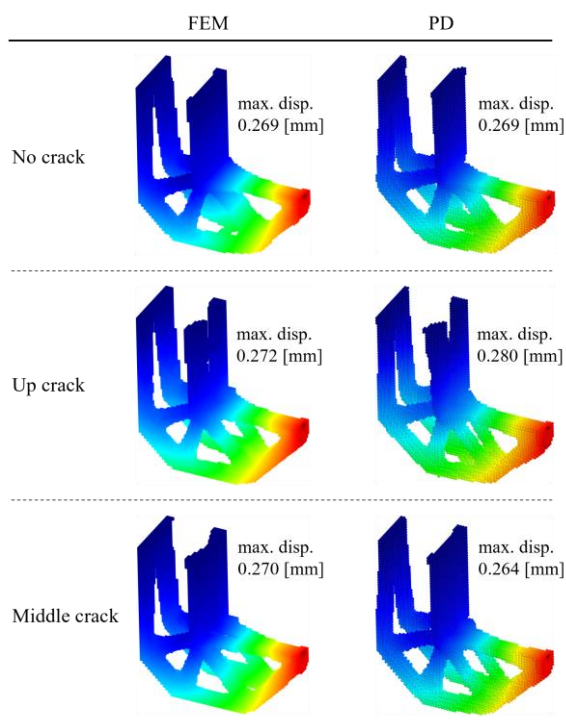

Fig 6. Total displacements for the topologies obtained by FEM-TO and PD-TO for varying crack scenarios.

4. Conclusions

In this research effort, we proposed a three-dimensional topology optimization procedure that utilizes a non-local analysis method namely peridynamics to initiate surface cracks realistically and easily into the selected regions. To better evaluate and validate the proposed framework, one of the most popular optimization tools FEM-TO is also utilized by modeling the same cracked scenarios. A comparison between the compliance results obtained by FEM-TO and PD-TO showed that PD-TO is a more viable method for optimizing the cracked structures. It is shown that FEM-TO is more prone to only open holes in the vicinity of the crack. Therefore, FEM-TO results brought more compliant structures. Observing the final topologies by considering the crack positions, it can be concluded that the PD-TO method is more sensitive to crack involvement. In the future, this study can be extended by a variety of problems and cracked scenarios to better analyze the effects of modeling and optimizing three-dimensional structures with defects. This modeling ability can be utilized to optimize the additively manufactured parts with their defects. In this way, the structures become more resistant to the previous process-induced cracks by considering them during optimization.

Author's statement
Conflict of interest: Authors state no conflict of interest. Informed consent: Informed consent has been obtained from all individuals included in this study. Ethical approval: n/a.

References
1. Yang, R.J. and Chahande, A.I., 1995. Automotive applications of topology optimization. Structural optimization, 9(3), pp.245-249.
2. Gersborg-Hansen, A., Sigmund, O. and Haber, R.B., 2005. Topology optimization of channel flow problems. Structural and multidisciplinary optimization, 30(3), pp.181-192.
3. Yoon, G.H., Jensen, J.S. and Sigmund, O., 2007. Topology optimization of acoustic–structure interaction problems using a mixed finite element formulation. International journal for numerical methods in engineering, 70(9), pp.1049-1075.
4. Cavazzuti, M., Baldini, A., Bertocchi, E., Costi, D., Torricelli, E. and Moruzzi, P., 2011. High performance automotive chassis design: a topology optimization based approach. Structural and Multidisciplinary Optimization, 44(1), pp.45-56.
5. Zhu, J.H., Zhang, W.H. and Xia, L., 2016. Topology optimization in aircraft and aerospace structures design. Archives of Computational Methods in Engineering, 23(4), pp.595-622.
6. Briot, S. and Goldsztejn, A., 2018. Topology optimization of industrial robots: Application to a five-bar mechanism. Mechanism and Machine Theory, 120, pp.30-56.

7. Rozvany, G.I., Zhou, M. and Birker, T., 1992. Generalized shape optimization without homogenization. Structural optimization, 4(3), pp.250-252.

8. Bendsøe, M.P. and Sigmund, O., 1999. Material interpolation schemes in topology optimization. Archive of applied mechanics, 69(9), pp.635-654.

9. Bendsoe, M.P. and Sigmund, O., 2003. Topology optimization: theory, methods, and applications. Springer Science & Business Media.

10. Xie, Y.M. and Steven, G.P., 1993. A simple evolutionary procedure for structural optimization. Computers & structures, 49(5), pp.885-896.

11. Huang, X. and Xie, Y.M., 2010. A further review of ESO type methods for topology optimization. Structural and Multidisciplinary Optimization, 41(5), pp.671-683.

12. Querin, O.M., Steven, G.P. and Xie, Y.M., 2000. Evolutionary structural optimisation using an additive algorithm. Finite elements in Analysis and Design, 34(3-4), pp.291-308.

13. Yang, X.Y., Xie, Y.M., Steven, G.P. and Querin, O.M., 1999. Bidirectional evolutionary method for stiffness optimization. AIAA journal, 37(11), pp.1483-1488.

14. Querin, O.M., Young, V., Steven, G.P. and Xie, Y.M., 2000. Computational efficiency and validation of bi-directional evolutionary structural optimisation. Computer methods in applied mechanics and engineering, 189(2), pp.559-573.

15. Huang, X., Xie, Y.M. and Burry, M.C., 2007. Advantages of bi-directional evolutionary structural optimization (BESO) over evolutionary structural optimization (ESO). Advances in Structural Engineering, 10(6), pp.727-737.

16. Zegard, T. and Paulino, G.H., 2015. GRAND3—Ground structure based topology optimization for arbitrary 3D domains using MATLAB. Structural and Multidisciplinary Optimization, 52(6), pp.1161-1184.

17. Wang, M.Y., Wang, X. and Guo, D., 2003. A level set method for structural topology optimization. Computer methods in applied mechanics and engineering, 192(1-2), pp.227-246.

18. Sethian, J.A. and Wiegmann, A., 2000. Structural boundary design via level set and immersed interface methods. Journal of computational physics, 163(2), pp.489-528.

19. Zhang, W., Chen, J., Zhu, X., Zhou, J., Xue, D., Lei, X. and Guo, X., 2017. Explicit three dimensional topology optimization via Moving Morphable Void (MMV) approach. Computer Methods in Applied Mechanics and Engineering, 322, pp.590-614.

20. Svanberg, K., 1987. The method of moving asymptotes—a new method for structural optimization. International journal for numerical methods in engineering, 24(2), pp.359-373.

21. Svanberg, K., 1993. The method of moving asymptotes (MMA) with some extensions. In Optimization of large structural systems (pp. 555-566). Springer, Dordrecht.

22. Mercelis, P. and Kruth, J.P., 2006. Residual stresses in selective laser sintering and selective laser melting. Rapid prototyping journal.

23. Bartlett, J.L. and Li, X., 2019. An overview of residual stresses in metal powder bed fusion. Additive Manufacturing, 27, pp.131-149.

24. Belytschko, T., Lu, Y.Y. and Gu, L., 1994. Element-free Galerkin methods. International journal for numerical methods in engineering, 37(2), pp.229-256.

25. Monaghan, J.J., 2012. Smoothed particle hydrodynamics and its diverse applications. Annual Review of Fluid Mechanics, 44, pp.323-346.

26. Silling, S.A., 2000. Reformulation of elasticity theory for discontinuities and long-range forces. Journal of the Mechanics and Physics of Solids, 48(1), pp.175-209.

27. Silling, S.A. and Askari, E., 2005. A meshfree method based on the peridynamic model of solid mechanics. Computers & structures, 83(17-18), pp.1526-1535.

28. Silling, S.A., Epton, M., Weckner, O., Xu, J. and Askari, E., 2007. Peridynamic states and constitutive modeling. Journal of elasticity, 88(2), pp.151-184.

29. Kefal, A., Sohouli, A., Oterkus, E., Yildiz, M. and Suleman, A., 2019. Topology optimization of cracked structures using peridynamics. Continuum Mechanics and Thermodynamics, 31(6), pp.1645-1672.

30. Sohouli, A., Kefal, A., Abdelhamid, A., Yildiz, M. and Suleman, A., 2020. Continuous density-based topology optimization of cracked structures using peridynamics. Structural and Multidisciplinary Optimization, 62(5), pp.2375-2389.

31. Lahe Motlagh, P. and Kefal, A., 2021. Comparative study of peridynamics and finite element method for practical modeling of cracks in topology optimization. Symmetry, 13(8), p.1407.

32. Motlagh, P. L., Kendibilir, A., Koc, B., & Kefal, A. (2021). Peridynamics-informed effect of micro-cracks on topology optimization of lightweight structures. Journal of Additive Manufacturing Technologies, 1(3), 610–610.

33. Kendibilir, A., Lahe motlagh, P., & Kefal, A. (2021). Three-Dimensional Topology Optimization for Marine Structure Components Using Non-Local Methods (pp. 49–55).

34. Hassani, B. and Hinton, E., 1998. A review of homogenization and topology optimization III—topology optimization using optimality criteria. Computers & structures, 69(6), pp.739-756.

35. Sigmund, O., 2001. A 99 line topology optimization code written in Matlab. Structural and multidisciplinary optimization, 21(2), pp.120-127.